Cycloruthenated Imines: A Step into the Nanomolar Region

Arsenii A. Vasil'ev , Ivan I. Troshin , Pavel G. Shangin , Ksenia M. Voroshilkina , Ilya A. Shutkov , Alexey A. Nazarov , Aleksei V. Medved'ko *

Posted Date: 9 December 2025

doi: 10.20944/preprints202512.0562.v1

Keywords: cycloruthenated complexes; imines; benzene; thiophene; cytotoxicity

 doi:10.20944/preprints202512.0562.v1

Article

Cycloruthenated Imines: A Step into the Nanomolar Region

Arsenii A. Vasil'ev [1,2], Ivan I. Troshin [1,3], Pavel G. Shangin [1], Ksenia M. Voroshilkina [2], Ilya A. Shutkov [2], Alexey A. Nazarov [2] and Aleksei V. Medved'ko [1,*]

[1] N.D. Zelinsky Institute of Organic Chemistry RAS, Moscow, Russia
[2] M.V. Lomonosov Moscow State University, Chemistry Department, Moscow, Russia
[3] MIREA-Russian Technological University, 78 Vernadsky Avenue, 119454 Moscow, Russia
* Correspondence: lexeym@gmail.com

Abstract

A new series of promising and easily accessible antiproliferative agents based on cycloruthenated imines of benzene and thiophene carbaldehydes has been developed and fully characterized using UV-Vis spectroscopy, X-ray diffraction, NMR, HRMS, and cyclic voltammetry. The biological activity of these compounds was tested against A2780, cisplatin-resistant A2780, and HEK293 cell lines, and they exhibited nanomolar IC_{50} values. They also showed a selectivity index of up to 2.5, indicating their potential as promising antiproliferative compounds.

Keywords: cycloruthenated complexes; imines; benzene; thiophene; cytotoxicity

1. Introduction

Despite global efforts to treat cancer, global mortality rates and newly diagnosed cancers continue to rise steadily. Malignant tumors remain a key factor limiting life expectancy. Chemotherapy is a traditional and widely used method of cancer treatment. Some of the most popular anticancer drugs are platinum compounds: cisplatin, carboplatin, and others. They have proven their effectiveness; however, despite their advantages, they can cause serious side effects, including hepatotoxicity, neurotoxicity, ototoxicity, and others [1,2]. Therefore, the scientific community is faced with the task of creating analogues of platinum compounds devoid of the above-mentioned drawbacks. Other transition metals, such as copper, iridium, osmium, gold, and ruthenium compounds, are being actively studied as anticancer agents [3,4]. Ruthenium is the most promising in this series, since it has broad coordination capabilities, unique mechanisms of anticancer activity in living cells, and its compounds are more accessible for commercial use than iridium or platinum precursors. Several families of anticancer drugs have already been developed based on ruthenium, including wide-layered complexes such as the NAMI type [5] and the RAPTA-type [6]. Photosensitizers based on ruthenium complexes can also be used for photodynamic cancer therapy [7,8]. A large number of ruthenium cyclometallic compounds containing a metal-carbon bond have been described in the literature. They are often used as dyes for DSSCs[9], as well as catalysts for oxidation [10] and cross-coupling [11]. At the same time, the literature also contains examples of the use of cycloruthenated complexes as anticancer drugs [12–21] Several years ago, we published a paper in which we synthesized ruthenium cyclometallic compounds containing a thiophene moiety [22]. A study of their anticancer properties showed that they are an order of magnitude more cytotoxic than the model drug cisplatin [23]. The role of substituents in the thiophene ring was studied, and it was shown that halogen substituents have virtually no effect on the IC_{50} values. However, the effect of substituents in the aniline fragment on cytotoxicity remains unexplored. Furthermore, it was necessary to study the effect of replacing the aldehyde moiety with the benzene moiety.

 doi:10.20944/preprints202512.0562.v1

2. Results and Discussion

2.1. Synthesis

All intermediate compounds and target complexes were obtained using methods similar to those described previously [23] (Scheme 1). Cycloruthenated complexes **3a**-**o** were synthesized with moderate to good yields by a two-step procedure by cyclometallation of imines and chelation of the resulting acetonitrile complexes **2a**-**o**. The remaining coordination sites were occupied by 2,2'-bipyridines to stabilize ruthenium in the (II) oxidation state, while aromatic ligands increase lipophilicity, facilitating transport across biological membranes. It is believed that ruthenium anticancer agents can bind to nuclear DNA via intercalation interactions; therefore, the presence of aromatic ligands enables stacking interactions between the ruthenium ring and nitrogenous base pairs.

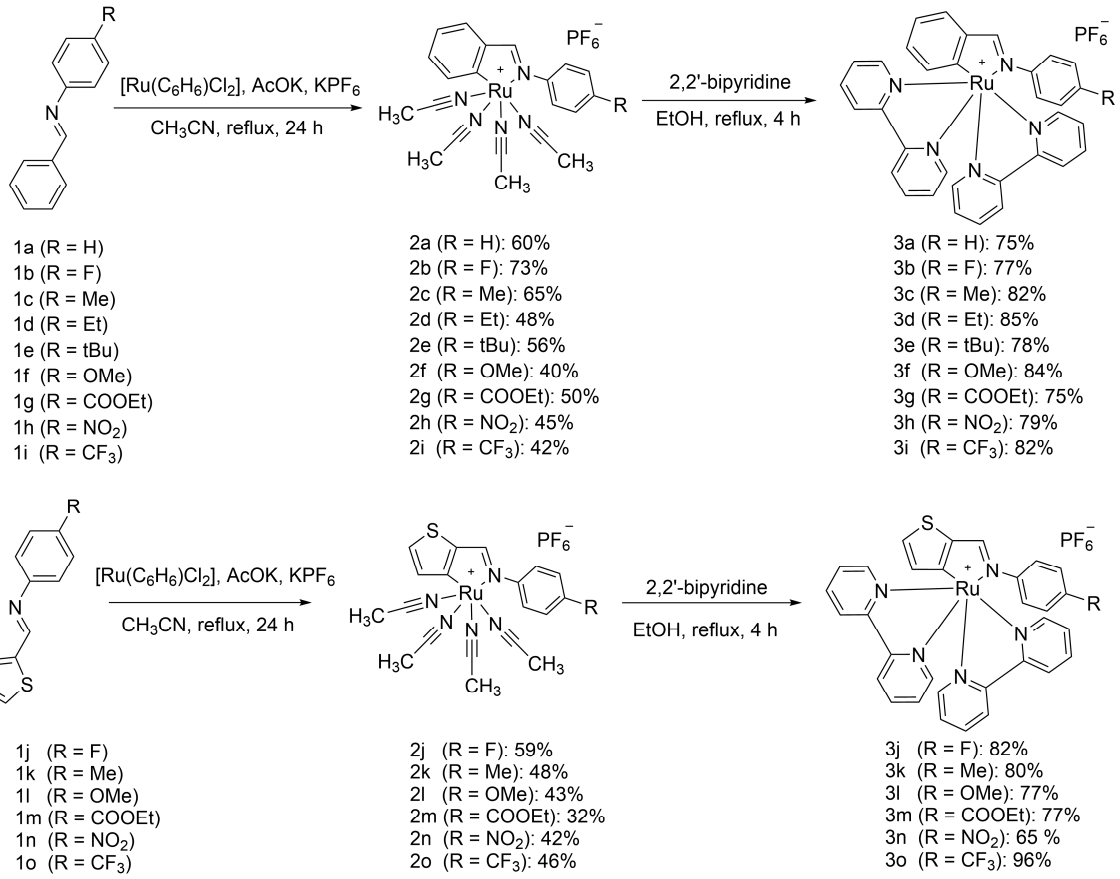

Scheme 1. Preparation of ruthenium complexes.

2.2. Crystallography

From a crystallographic point of view, the obtained complexes have a similar structure (Table S1, Figs S30-S51). Thus, the lengths of the Ru-C bonds are in the range of 2.008-2.032 Å, Ru-N(aniline) - 2.062 - 2.123 Å, Ru-N, located opposite the Ru-C bond - 2.132-2.172 Å (Table 1). The plane of the aniline ring is inclined relative to the plane of the five-membered ring with the ruthenium atom with the dihedral angle 40.65 - 65.66 °. The sign of this angle is not characteristic, either for acetonitrile, or for bipyridine complexes. It is worth noting that the formation of the bipyridine complex decreases the modulus of the dihedral angle by an average of 10 ° (cf. **2a** and **3a**, **2b** and **3b**, **2e** and **3e**, **2f** and **3f**). In bipyridine complexes, one fragment is more distorted than the other. The dihedral angle between the two pyridine rings ranges from 1.85° to 10.77°. The dihedral angle of the second fragment is approximately 1°.

 doi:10.20944/preprints202512.0562.v1

Table 1. Selected bond lengths and angles of ruthenium complexes.

	Aniline-(Ru-N) Dihedral Angle, °	Py-Py Dihedral Angle, °	Ru-N(aniline), Å	Ru-N, Å [a]	Ru-C, Å
2a (H)	+65.66		2.071	2.151	2.026
2b (F)	+58.36		2.065	2.155	2.035
2d (Et)	-52.43		2.069	2.142	2.027
2e (tBu)	-57.51		2.069	2.155	2.025
2f (OMe)	-61.74		2.066	2.152	2.019
2g (CO_2Et)[b]	-51.97		2.062	2.158	2.023
	+40.65		2.079	2.159	2.017
2h (NO_2)[b]	+42.47		2.096	2.157	2.019
	+41.62		2.071	2.172	2.008
2i (CF_3)	-51.20		2.063	2.153	2.022
2j (F)	-47.59		2.102	2.139	2.019
2k (Me)	-49.30		2.096	2.136	2.022
2l (OMe) [b]	+52.94		2.093	2.132	2.018
	+41.76		2.114	2.139	2.015
2n (NO_2)	-47.17		2.105	2.140	2.020
3a (H)	+45.61	4.22	2.111	2.146	2.031
3b (F)	+49.65	1.85	2.104	2.136	2.030
3c (Me)	+39.77	5.01	2.117	2.152	2.031
3e (tBu)	+48.29	7.07	2.085	2.146	2.029
3f (OMe)	-55.21	3.52	2.063	2.155	2.036
3h (NO_2)	-52.22	3.96	2.091	2.156	2.031
3j (F)	+43.78	8.91	2.123	2.137	2.025
3l (OMe)	+48.94	10.77	2.117	2.148	2.010
3m (CO_2Et)	-58.58	5.47	2.110	2.137	2.018
3o (CF_3)	+55.99	3.79	2.106	2.127	2.019

[a] located opposite the Ru-C bond. [b] two independent molecules.

2.3. UV-vis Examination

UV spectra were recorded for complexes **3a–3o** in acetonitrile (Fig. 1) to determine their optical properties. All absorption spectra in acetonitrile exhibit two intensity bands: 250–300 nm (corresponding to the absorption bands of aromatic systems) and 450–600 nm (arising after metal coordination with 2,2'-bipyridine). This can be visually observed: during the reaction, acetonitriles are replaced by bipyridines, and the compounds change from orange to dark purple.

 doi:10.20944/preprints202512.0562.v1

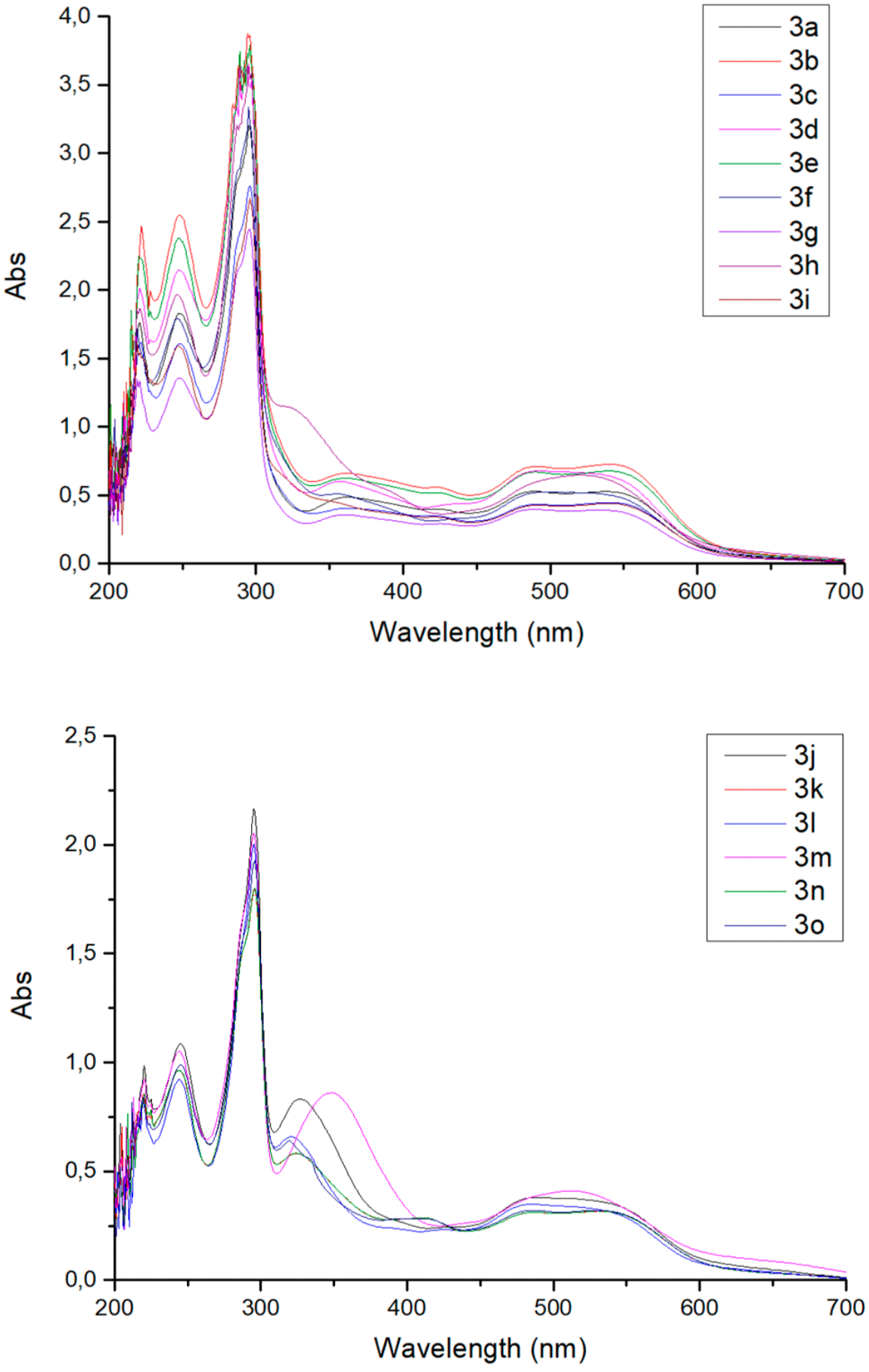

Figure 1. UV-vis spectra of **3a**-**3o** in acetonitrile, concentration 3.4*10^{-5} M.

 doi:10.20944/preprints202512.0562.v1

Stability of **3a**-**o** was also assessed in 0.5% DMSO solution in aqueous phosphate buffer (pH 7.4, 37 °C, 100 μM NaCl, 77.4 μM Na2HPO4, 22.6 μM NaH2PO4) or saline by comparing the UV spectrum of solutions of complexes 3a-o, recorded immediately after solution preparation, and the UV spectrum of the same solution after 18 h of incubation at room temperature (Figs S52-S53). The spectra were compatible for all the complexes, indicating that they were sufficiently stable. A slight change in the intensity of signals is due to the slow degradation of ruthenium complexes with the formation of aqua- and oxo-complexes, as well as partial precipitation, which is typical for ruthenium compounds [24].

2.4. Electrochemistry

The introduction of electron-withdrawing substituents increases the $E^{1/2}_{ox1}$ value of the Ru^{2+}/Ru^{3+} transition by an average of 40-60 mV (Table 2). The electron-donating methoxy group (**3f** and **3l**) weakly reduces this potential. When comparing the nitro group in the thiophene ring [23] with the nitro group in the aniline ring, the latter shifts the oxidation potential less strongly (257 mV vs 215 mV). Overall, the oxidation potentials for the phenyl and thiophene derivatives are close to each other, except for the ethoxycarbonyl derivatives **3g** and **3m**, for which the potential differs by almost a factor of two.

Table 2. The $E^{1/2}$ values (mV vs. Fc/Fc^+) of reduction and oxidation of the studied compounds in 0.1 M Bu_4NPF_6/MeCN were determined as the half-sum of the potentials of the forward and reverse peaks of the CV curves recorded for solutions with a concentration of 2.5 10^{-3} M at a potential scan rate of 100 mV s^{-1} on a glassy carbon working electrode at 298 K (for irreversible processes marked with an asterisk, the peak potentials are given).

	$E_p\ (E^{1/2}_{red2}), mV$	$E_p\ (E^{1/2}_{red1}), mV$	$E_p\ (E^{1/2}_{ox1}), mV$	$E_p\ (E^{1/2}_{ox2}), mV$	Additional peaks
3a (H)	-2277 (-2234)	-2022 (-1981)	139 (95)	1565	
3b (F)	-2264 (-2219)	-2010 (-1969)	155 (111)	1607	-2828
3c (Me)	-2015 (-1973)	-2268 (-2226)	144 (99)	1570	
3d (Et)	-2278 (-2233)	-2020 (-1981)	136 (92)	1551	-2905
3e (tBu)	-2280 (-2236)	-2026 (-1984)	128 (88)	1556	-2864
3f (OMe)	-2277 (-2235)	-2022 (-1984)	117 (78)	1352	
3g[a] (CO_2Et)	-2242	-2009 (-1961)	189 (135)	1635	-2551 (C=O reduction)
3h[b] (NO_2)	-	-	200 (161)	1679	-1507 (-1467) -NO_2 reduction -1970
3i (CF_3)	-2245 (-2198)	-1996 (-1959)	181 (139)	1611	-2640 (C-F cleavage)
3j (F)	-2245 (-2202)	-1997 (-1956)	145 (102)	1422	
3k (Me)	-2253 (-2213)	-2002 (-1962)	117 (77)	1364	-2909
3l (OMe)	-2256 (-2216)	-2003 (-1962)	107 (70)	1183 (1129)	-2874 (shoulder)
3m[c] (CO_2Et)	-2226 (-2167)	-1989 (-1931)	78 (127)	1517	-2582 (C=O reduction)
3n[d] (NO_2)	-	-	215 (165)	1545	-1534 (-1488) (-NO_2 reduction)
3o (CF_3)	-2213 (-2175)	-1976 (-1936)	181 (143)	1460	-2582 (C-F cleavage)

 doi:10.20944/preprints202512.0562.v1

[a] C=O reduction is reversible, but too distorted, also affects $E_{red1}^{1/2}$ peak reversibility. [b] After first reduction of -NO_2 further curve is uninterpretable. [c] C=O reduction is reversible, but too distorted. [d] Very distorted $E_{red2}^{1/2}$ and $E_{red1}^{1/2}$.

2.5. Biological Study

The *in vitro* antiproliferative activity of the synthesized Ru-organometallic compounds and several starting ligands was evaluated against three human cell lines using the MTT assay. We selected a small panel of cell lines that provided insights into the efficacy and potential therapeutic utility of the compounds. The panel includes the A2780 human ovarian carcinoma cell line, which is sensitive to cisplatin, its cisplatin-resistant counterpart, A2780cis, also a non-malignant human embryonic kidney cell line, HEK293. The use of A2780 and A2780cis paired cell lines allowed us to directly assess the ability of the compounds to overcome resistance mechanisms. The inclusion of the HEK293 cell line can give us preliminary indication of selectivity against non-cancerous cells. Cisplatin, a clinically used drug, was used as a positive control in all experiments. All studies were performed in triplicate and repeated in three independent experiments. The results, expressed as the half-maximal inhibitory concentration after 72 h incubation (IC_{50}), are summarized in Table 3.

Table 3. Antiproliferative activity of ruthenium complexes with thiophene-based imines **2a-e**, ligands **S4a-e** and cisplatin against various human cancer cells R_f showed resistance coefficient (calculated as IC_{50} on A2780cis divided on IC_{50} on A2780 cell line). The results are the mean values ± SD of three independent experiments, each of which was done in triplicate. The Selectivity Index is calculated as IC50 on HEK293 divided on IC_{50} on A2780 cell line.

	IC_{50} (72 h)/nM				
Compound	**A2780**	**A2780Cis**	**Rf**	**HEK293**	**Selectivity Index, SI**
Cisplatin	2640±350	1560±210	5.9	22000±4000	8.3
3b (F)	90 ± 30	250 ± 60	2.8	100 ± 30	1.1
3c (Me)	70 ± 6	120 ± 10	1.7	70 ± 10	1.0
3d (Et)	45 ± 5	150 ± 10	3.3	80 ± 10	1.8
3e (*t*Bu)	70 ± 30	170 ± 30	2.4	68 ± 6	1.0
3f (OMe)	65 ± 4	120 ± 40	1.8	64 ± 7	1.0
3g (CO_2Et)	100 ± 20	230 ± 20	2.3	140 ± 20	1.4
3h (NO_2)	250 ± 30	760 ± 80	3.0	370 ± 80	1.5
3i (CF_3)	80 ± 10	240 ± 20	3.0	107 ± 8	1.3
3j (F)	43±3	91±9	2.1	60 ± 10	1.4
3k (Me)	30±2	10±0.4	0.3	70 ± 30	2.3
3l (OMe)	39±3	39±10	1.0	40 ± 10	1.0
3m (CO_2Et)	57±20	84±12	1.5	140 ± 10	2.5
3n (NO_2)	270±4	960±100	3.6	530 ± 30	2.0
3o (CF_3)	96±3	150±5	6.4	160 ± 30	1.7
1b (F)	> 200000	> 100000	-	21610	-
1f (OMe)	> 200000	> 100000	-	> 200000	-
1g (CO_2Et)	42090	> 100000	-	25430	-

Based on the initial analysis of the data, we can conclude that the IC_{50} values for all Ru compounds fall within the medium to high nanomolar range, suggesting a high level of cytotoxicity against both malignant and non-malignant cells. Moreover, the organometallic compounds appear to be several times more cytotoxic than cisplatin, approximately 10 times or more, although their selectivity for cancer cells is only moderate. The selectivity index for these compounds does not exceed 2.5, compared to 8.3 for cisplatin.

 doi:10.20944/preprints202512.0562.v1

The presence of a ruthenium atom in a complex determines its biological activity. The data show that ligands such as **1b**, **1f**, and **1g** do not exhibit any cytotoxicity, but the cytotoxicity of N-benzylideneaniline complexes (**3b-i**) and thiophenylimine compounds (**3j-o**) against A2780 is virtually identical. On the other hand, thiophenylidenimine ruthenacycles (against A2780cis) are several times more cytotoxic than N-benzylideneaniline complexes. This makes them a promising treatment for cisplatin-resistant tumors.

If we look at the structure of the ligands, we can draw the following conclusions about their activity: the electron-donating OMe group slightly increases cytotoxicity, while the acceptors NO_2 and CF_3 reduce cytotoxicity. At the same time, alkyl substituents (except for *t*Bu) increase the cytotoxicity of both the benzylideneaniline and thiophenylidenimine families of complexes. This can be attributed to their increased lipophilicity.

3. Experimental Section

3.1. General Procedure for Compounds 2a-2o.

Imine **1** (0.40 mmol, 2 eq) dissolved in acetonitrile (15 ml) was added to a three-necked flask equipped with a reflux condenser with $[Ru(C_6H_6)Cl_2]_2$ (0.20 mmol, 1 eq), potassium hexafluorophosphate (0.80 mmol, 4 eq), potassium acetate (0.60 mmol, 3 eq) and refluxed in an argon atmosphere for 24 hours. The reaction mixture was evaporated, residue was dissolved in DCM (15 ml) and of water (10 ml), organic layer was separated, aqueous layer was washed with DCM (5 ml), organic phases were combined, dried over sodium sulfate and evaporated to dryness. Crude product was purified with column chromatography on silica gel ($CHCl_3$:CH_3CN 10:1). Crystals suitable for X-ray analysis were grown by diethyl ether vapor diffusion on acetonitrile solution of complexes.

Tetrakis(acetonitrile)[N-((phenyl-κC²)methyliden]aniline-κN]ruthenium(II) hexafluorophosphate (**2a**).

Orange powder. Yield 60%.

^{1}H NMR (300 MHz, Acetonitrile-d_3) δ 8.46 (s, 1H), 8.03 (d, J = 7.5 Hz, 1H), 7.64 (dd, J = 7.5, 1.1 Hz, 1H), 7.49 – 7.42 (m, 2H), 7.39 – 7.34 (m, 1H), 7.34 – 7.28 (m, 2H), 7.13 (td, J = 7.4, 1.5 Hz, 1H), 6.96 (td, J = 7.3, 1.2 Hz, 1H), 2.51 (s, 3H), 2.12 (s, 6H), 1.96 (s, 3H).

^{13}C NMR (76 MHz, Acetonitrile-d_3): 191.61, 176.62, 152.09, 149.52, 138.15, 129.68, 128.76, 126.63, 124.03, 122.69, 121.81, 120.57, 117.35, 65.30, 14.66, 3.41, 2.93.

HRMS-ESI: calc for $[C_{19}H_{19}N_4Ru\text{-}CH_3CN]^+$ 405.0647, found 405.0643

Tetrakis(acetonitrile)[N-((phenyl-κC²)methyliden]-4-fluoroaniline-κN]ruthenium(II) hexafluorophosphate (**2b**).

Orange powder. Yield 73%.

^{1}H NMR (300 MHz, Acetonitrile-d_3) δ 8.45 (s, 1H), 8.02 (d, J = 7.5 Hz, 1H), 7.63 (d, J = 7.4 Hz, 1H), 7.35 – 7.28 (m, 2H), 7.22 – 7.10 (m, 3H), 6.96 (t, J = 7.3 Hz, 1H), 2.51 (s, 3H), 2.12 (s, 6H), 1.96 (s, 3H).

^{13}C NMR (151 MHz, Acetonitrile-d_3): 191.83, 176.98, 162.05, 160.44, 149.45, 148.55, 138.21, 129.83, 128.73, 124.55, 121.91, 120.63, 117.40, 115.22, 3.41, 2.94.

HRMS-ESI: calc for $[C_{19}H_{18}FN_{14}Ru\text{-}CH_3CN]^+$ 423.0534, found 423.0568.

Tetrakis(acetonitrile)[N-((phenyl-κC²)methyliden]-4-methylaniline-κN]ruthenium(II) hexafluorophosphate (**2c).**

Orange powder. Yield 65%.

^{1}H NMR (300 MHz, Acetonitrile-d_3) δ 8.43 (s, 1H), 8.01 (d, J = 7.5 Hz, 1H), 7.61 (dd, J = 7.5, 1.1 Hz, 1H), 7.26 (d, J = 8.3 Hz, 2H), 7.19 (d, J = 8.4 Hz, 2H), 7.12 (td, J = 7.4, 1.5 Hz, 1H), 6.96 (td, J = 7.3, 1.1 Hz, 1H), 2.51 (s, 3H), 2.39 (s, 3H), 2.11 (s, 6H), 1.96 (s, 3H).

^{13}C NMR (151 MHz, Acetonitrile-d_3): 191.40, 176.19, 149.80, 138.14, 136.59, 129.52, 129.20, 128.53, 123.97, 122.54, 121.76, 120.57, 117.36, 20.11, 3.45, 2.96.

HRMS-ESI: calc for $[C_{20}H_{21}N_4Ru\text{-}CH_3CN]^+$ 419.0822, found 419.0814.

Tetrakis(acetonitrile)[N-((phenyl-κC²)methyliden]-4-ethylaniline-κN]ruthenium(II) hexafluorophosphate (**2d**)

 doi:10.20944/preprints202512.0562.v1

Orange powder. Yield 48%.

^{1}H NMR (300 MHz, Acetonitrile-d_3) δ 8.44 (s, 1H), 8.01 (d, J = 7.5 Hz, 1H), 7.63 – 7.58 (m, 1H), 7.29 (d, J = 8.2 Hz, 2H), 7.21 (d, J = 8.3 Hz, 2H), 7.12 (t, J = 7.3 Hz, 1H), 6.96 (t, J = 7.3 Hz, 1H), 2.70 (q, J = 7.6 Hz, 2H), 2.51 (s, 3H), 2.12 (s, 6H), 1.96 (s, 3H), 1.26 (t, J = 7.6 Hz, 3H).

^{13}C NMR (151 MHz, Acetonitrile-d_3): 191.39, 176.22, 149.97, 149.58, 143.02, 138.14, 129.54, 128.55, 128.08, 123.98, 122.63, 121.77, 120.57, 117.36, 28.10, 15.25, 3.44, 2.97.

HRMS-ESI: calc for $[C_{21}H_{23}N_4Ru\text{-}CH_3CN]^+$ 433.1210, found 433.1215

Tetrakis(acetonitrile)[N-((phenyl-κC^2)methyliden]-4-(tert-butyl)aniline-κN]ruthenium(II) hexafluorophosphate (**2e**).

Orange powder. Yield 56%.

^{1}H NMR (300 MHz, Acetonitrile-d_3) δ 8.45 (s, 1H), 8.01 (d, J = 7.4 Hz, 1H), 7.62 (d, J = 7.4 Hz, 1H), 7.48 (d, J = 8.5 Hz, 2H), 7.24 (d, J = 8.4 Hz, 2H), 7.12 (t, J = 7.3 Hz, 1H), 6.96 (t, J = 7.3 Hz, 1H), 2.51 (s, 3H), 2.12 (s, 6H), 1.96 (s, 3H), 1.37 (s, 9H).

^{13}C NMR (151 MHz, Acetonitrile-d_3): 191.43, 176.25, 149.73, 138.15, 129.57, 128.57, 125.58, 124.00, 122.31, 121.79, 120.59, 117.38, 34.30, 30.68, 3.43, 2.96.

HRMS-ESI: calc for $[C_{23}H_{27}N_4Ru\text{-}CH_3CN]^+$ 315.6547, found 315.6548.

Tetrakis(acetonitrile)[N-((phenyl-κC^2)methyliden]-4-methoxyaniline-κN]ruthenium(II) hexafluorophosphate (**2f**).

Orange powder. Yield 40%.

^{1}H NMR (300 MHz, Acetonitrile-d_3) δ 8.42 (s, 1H), 8.01 (d, J = 7.5 Hz, 1H), 7.61 (d, J = 7.4 Hz, 1H), 7.26 (d, J = 8.8 Hz, 2H), 7.11 (t, J = 7.3 Hz, 1H), 7.00 – 6.92 (m, 3H), 3.84 (s, 3H), 2.51 (s, 3H), 2.11 (s, 6H), 1.96 (s, 3H).

^{13}C NMR (151 MHz, Acetonitrile-d_3): 191.19, 175.85, 158.52, 149.61, 145.56, 138.10, 129.41, 128.45, 123.79, 121.74, 120.57, 117.36, 113.75, 55.28, 2.99.

HRMS-ESI: calc for $[C_{19}H_{18}N_4ORu]^+$ 419.0812, found 419.0814.

Tetrakis(acetonitrile)[N-((phenyl-κC^2)methyliden]-4-ethoxycarbonylaniline-κN]ruthenium(II) hexafluorophosphate (**2g**).

Orange powder. Yield 50%.

^{1}H NMR (300 MHz, Acetonitrile-d_3) δ 8.50 (s, 1H), 8.10 – 8.02 (m, 3H), 7.67 (d, J = 7.3 Hz, 1H), 7.38 (d, J = 8.4 Hz, 2H), 7.14 (t, J = 7.4 Hz, 1H), 6.98 (t, J = 7.3 Hz, 1H), 4.37 (q, J = 7.1 Hz, 2H), 2.52 (s, 3H), 2.12 (s, 6H), 1.96 (s, 3H), 1.38 (t, J = 7.1 Hz, 3H).

^{13}C NMR (151 MHz, Acetonitrile-d_3): 192.72, 177.59, 165.84, 155.89, 149.44, 138.28, 130.31, 130.03, 128.98, 124.23, 123.06, 122.02, 120.71, 117.38, 61.00, 13.68, 3.45, 2.96.

HRMS-ESI: calc for $[C_{22}H_{23}N_4O_2Ru\text{-}CH_3CN]^+$ 477.0853, found 477.0859.

Tetrakis(acetonitrile)[N-((phenyl-κC^2)methyliden]-4-nitroaniline-κN]ruthenium(II) hexafluorophosphate (**2h**).

Orange powder. Yield 45%.

^{1}H NMR (300 MHz, Acetonitrile-d_3) δ 8.54 (s, 1H), 8.33 – 8.27 (m, 2H),

8.06 (d, J = 7.5 Hz, 1H), 7.71 (dd, J = 7.5, 1.1 Hz, 1H), 7.51 – 7.46 (m, 2H), 7.16 (td, J = 7.3, 1.4 Hz, 1H), 6.99 (td, J = 7.4, 1.1 Hz, 1H), 2.52 (s, 3H), 2.13 (s, 6H), 1.96 (s, 3H).^{13}C NMR (151 MHz, Acetonitrile-d3): 193.64, 178.56, 157.44, 149.33, 146.21, 138.35, 130. 82, 129.27, 124.44, 123.99, 122.18, 120.82, 117.37, 3.46, 2.99.

HRMS-ESI: calc for $[C_{19}H_{18}N_5O_2Ru\text{-}CH_3CN]^+$ 435.0765, found 435.0766.

Tetrakis(acetonitrile)[N-((phenyl-κC^2)methyliden]-4-(trifluoromethyl)aniline-κN]ruthenium(II) hexafluorophosphate (**2i**).

Orange powder. Yield 42%.

^{1}H NMR (300 MHz, Acetonitrile-d_3) δ 8.51 (s, 1H), 8.04 (d, J = 7.5 Hz, 1H), 7.77 (d, J = 8.4 Hz, 2H), 7.68 (d, J = 7.5 Hz, 1H), 7.46 (d, J = 8.3 Hz, 2H), 7.15 (t, J = 7.4 Hz, 1H), 6.98 (t, J = 7.4 Hz, 1H), 2.52 (s, 3H), 2.12 (s, 6H), 1.96 (s, 3H).

^{13}C NMR (151 MHz, Acetonitrile-d_3): 192.73, 177.99, 155.22, 149.38, 138.29, 130.39, 129.05, 126.01, 124.27, 123.64, 122.06, 120.74, 117.37, 3.46, 2.99.

 doi:10.20944/preprints202512.0562.v1

HRMS-ESI: calc for $[C_{20}H_{18}F_3N_4Ru\text{-}CH_3CN]^+$ 473.0528, 473.0524.

Tetrakis(acetonitrile)[N-((thiophene-2-yl-κC²)methyliden]-4-fluoroaniline-κN]ruthenium(II) hexafluorophosphate (**2j**).

Orange powder. Yield 59 %.

^{1}H NMR (300 MHz, Acetonitrile-d_3) δ 8.38 (s, 1H), 7.82 (d, J = 4.6 Hz, 1H), 7.63 (d, J = 4.1 Hz, 1H), 7.34 – 7.27 (m, 2H), 7.20 – 7.13 (m, 2H), 2.51 (s, 3H), 2.12 (s, 6H), 1.96 (s, 3H).

^{13}C NMR (76 MHz, Acetonitrile-d_3) δ 202.67, 168.15, 163.47, 160.26, 149.81, 149.78, 138.48, 137.04, 134.08, 125.66, 125.55, 125.23, 123.44, 116.33, 116.04, 31.61, 30.35, 4.32, 3.89, 1.77.

HRMS-ESI: calc for $[C_{19}H_{19}BrN_5RuS\text{-}CH_3CN]^+$ 470.0387, found 470.0397

Tetrakis(acetonitrile)[N-((thiophene-2-yl-κC²)methyliden]-4-methylaniline-κN]ruthenium(II) hexafluorophosphate (**2k).**

Orange powder. Yield 48 %.

^{1}H NMR (300 MHz, Acetonitrile-d_3) δ 8.38 (s, 1H), 7.80 (d, J = 4.6 Hz, 1H), 7.62 (d, J = 4.6 Hz, 1H), 7.25 – 7.16 (m, 4H), 2.51 (s, 3H), 2.38 (s, 3H), 2.12 (s, 6H), 1.96 (s, 3H).

^{13}C NMR (75 MHz, Acetonitrile-d_3) δ 201.70, 167.47, 151.03, 138.48, 136.98, 136.91, 133.58, 130.16, 125.11, 123.73, 123.29, 21.05, 4.34, 3.91, 1.77.

HRMS-ESI: calc for $[C_{19}H_{19}BrN_5RuS\text{-}CH_3CN]^+$ 425.0372, found 425.0362.

Tetrakis(acetonitrile)[N-((thiophene-2-yl-κC²)methyliden]-4-methoxyaniline-κN]ruthenium(II) hexafluorophosphate (**2l**).

Orange powder. Yield 43 %.

^{1}H NMR (300 MHz, Acetonitrile-d_3) δ 8.39 (s, 1H), 7.82 (d, J = 4.6 Hz, 1H), 7.64 (d, J = 4.6 Hz, 1H), 7.30 – 7.23 (m, 2H), 7.02 – 6.96 (m, 2H), 3.86 (s, 3H), 2.54 (s, 3H), 2.14 (s, 6H), 1.99 (s, 3H).

^{13}C NMR (76 MHz, Acetonitrile-d_3) δ 201.18, 167.17, 159.05, 146.78, 138.41, 136.93, 133.36, 132.27, 129.73, 125.06, 124.87, 123.27, 114.69, 56.19, 4.34, 3.92.

HRMS-ESI: calc for $[C_{19}H_{19}BrN_5RuS\text{-}CH_3CN]^+$ 482.0587, found 482.0595.

Tetrakis(acetonitrile)[N-((thiophene-2-yl-κC²)methyliden]-4-ethoxycarbonylaniline-κN]ruthenium(II) hexafluorophosphate (**2m**).

Orange powder. Yield 32 %.

^{1}H NMR (300 MHz, Acetonitrile-d_3) δ 8.45 (s, 1H), 8.05 (d, J = 8.5 Hz, 2H), 7.88 (d, J = 4.7 Hz, 1H), 7.66 (d, J = 4.7 Hz, 1H), 7.39 (d, J = 8.4 Hz, 2H), 4.36 (q, J = 7.1 Hz, 2H), 2.52 (s, 3H), 2.12 (s, 6H), 1.96 (s, 3H), 1.38 (t, J = 7.1 Hz, 3H).

^{13}C NMR (76 MHz, Acetonitrile-d_3) δ 204.97, 168.66, 166.87, 157.31, 138.94, 137.13, 135.02, 130.96, 129.02, 125.33, 124.17, 123.56, 61.85, 14.63, 4.37, 3.92.

HRMS-ESI: calc for $[C_{19}H_{19}BrN_5RuS\text{-}CH_3CN]^+$ 524.0694, found 524.0695.

Tetrakis(acetonitrile)[N-((thiophene-2-yl-κC²)methyliden]-4-nitroaniline-κN]ruthenium(II) hexafluorophosphate (**2n**).

Orange powder. Yield 42 %.

^{1}H NMR (300 MHz, Acetonitrile-d_3) δ 8.50 (s, 1H), 8.27 (d, J = 9.0 Hz, 2H), 7.92 (d, J = 4.7 Hz, 1H), 7.68 (d, J = 4.7 Hz, 1H), 7.49 (d, J = 9.0 Hz, 2H), 2.52 (s, 3H), 2.12 (s, 6H), 1.96 (s, 3H).

^{13}C NMR (76 MHz, Acetonitrile-d_3) δ 207.50, 169.44, 159.04, 146.53, 139.30, 137.28, 136.07, 125.48, 125.39, 124.97, 123.77, 31.59, 30.34, 4.37, 3.94, 1.77.

HRMS-ESI: calc for $[C_{19}H_{19}BrN_5RuS\text{-}CH_3CN]^+$ 497.0332, found 497.0344.

Tetrakis(acetonitrile)[N-((thiophene-2-yl-κC²)methyliden]-4-(trifluoromethyl)aniline-κN]ruthenium(II) hexafluorophosphate (**2o**).

Orange powder. Yield 46 %.

^{1}H NMR (300 MHz, Acetonitrile-d_3) δ 8.46 (s, 1H), 7.88 (d, J = 4.6 Hz, 1H), 7.74 (d, J = 8.3 Hz, 2H), 7.66 (d, J = 4.6 Hz, 1H), 7.46 (d, J = 8.2 Hz, 2H), 2.52 (s, 3H), 2.12 (s, 6H), 1.96 (s, 3H).

^{13}C NMR (76 MHz, Acetonitrile-d_3) δ 205.10, 169.01, 156.59, 138.89, 137.13, 135.13, 128.29, 127.86, 126.88 (q, J = 3.8 Hz), 125.36, 124.75, 123.60, 4.38, 3.94.

HRMS-ESI: calc for $[C_{19}H_{19}BrN_5RuS\text{-}CH_3CN]^+$ 520.0356, found 520.0367.

 doi:10.20944/preprints202512.0562.v1

3.1. General Procedure for Compounds 3a-3o.

Complex **2** (0.30 mmol, 1 eq) and 2,2′-bipyridine (0.60 mmol, 2 eq) were introduced into a flask equipped with a reflux condenser, ethanol (18 ml) was added, and the mixture was refluxed in an argon atmosphere for 4 hours. The reaction mixture was evaporated and purified with column chromatography on silica gel ($CHCl_3$:CH_3CN 10:1). The product was dissolved in minimal volume of CH_3CN and added dropwise to large excess of diethyl ether under vigorous stirring. The precipitate was filtered, washed with diethyl ether and dried in vacuo for 3 h. Crystals suitable for X-ray analysis were grown by diethyl ether vapor diffusion on acetonitrile solution of complexes.

Bis(2,2′-bipiridine)[N-((phenyl-κC^2)methyliden]aniline-κN]ruthenium(II) hexafluorophosphate (**3a**).

Dark purple powder. Yield 75%.

^{1}H NMR (300 MHz, Acetonitrile-d_3) δ 8.73 (s, 1H), 8.63 (d, *J* = 5.7 Hz, 1H), 8.33 (d, *J* = 8.2 Hz, 2H), 8.13 (d, *J* = 8.2 Hz, 1H), 8.00 (dd, *J* = 12.8, 6.9 Hz, 2H), 7.84 (p, *J* = 7.7 Hz, 3H), 7.78 – 7.64 (m, 4H), 7.40 (t, *J* = 6.6 Hz, 1H), 7.31 (t, *J* = 6.6 Hz, 1H), 7.19 (t, *J* = 6.5 Hz, 2H), 7.02 – 6.81 (m, 5H), 6.53 (dd, *J* = 12.5, 7.3 Hz, 3H).

^{13}C NMR (151 MHz, Acetonitrile-d_3): 201.76, 176.18, 158.78, 158.01, 157.64, 155.56, 155.43, 153.29, 151.82, 151.24, 150.07, 149.36, 136.77, 136.36, 136.09, 135.10, 134.81, 131.82, 130.09, 129.47, 127.43, 127.39, 127.35, 127.16, 127.05, 124.02, 123.67, 123.21, 122.64, 121.63.

CHN calc. for $C_{33}H_{26}N_5RuPF_6$*0.2$C_4H_{10}O$: C: 53.29; H: 3.53; N: 9.31. Obs. C: 53.29; H: 3.52; N: 9.39.

Bis(2,2′-bipiridine)[N-((phenyl-κC^2)methyliden]-4-fluoroaniline-κN]ruthenium(II) hexafluorophosphate (**3b**).

Dark purple powder. Yield 77%.

^{1}H NMR (300 MHz, Acetonitrile-d_3) δ 8.72 (s, 1H), 8.59 (d, *J* = 5.7 Hz, 1H), 8.34 (d, *J* = 8.1 Hz, 2H), 8.15 (d, *J* = 8.1 Hz, 1H), 8.05 (d, *J* = 8.2 Hz, 1H), 7.96 (d, *J* = 5.6 Hz, 1H), 7.84 (p, *J* = 7.2 Hz, 3H), 7.78 – 7.70 (m, 3H), 7.66 (d, *J* = 5.3 Hz, 1H), 7.39 (t, *J* = 6.6 Hz, 1H), 7.31 (t, *J* = 6.7 Hz, 1H), 7.20 (q, *J* = 6.2 Hz, 2H), 6.87 (p, *J* = 7.4 Hz, 2H), 6.66 (t, *J* = 8.7 Hz, 2H), 6.58 – 6.47 (m, 3H).

^{13}C NMR (151 MHz, Acetonitrile-d_3): 200.85, 175.57, 161.43, 159.82, 157.77, 157.04, 156.67, 154.49, 152.32, 150.34, 149.15, 148.33, 147.22, 135.94, 135.21, 134.22, 133.92, 130.96, 129.22, 126.58, 123.49, 122.37, 120.73, 117.38, 115.10.

CHN calc. for $C_{33}H_{25}N_5RuPF_7$: C: 52.39; H: 3.33; N: 9.26. Obs. C: 52.23; H: 3.21; N: 9.09.

Bis(2,2′-bipiridine)[N-((phenyl-κC^2)methyliden]-4-methylaniline-κN]ruthenium(II) hexafluorophosphate (**3c**).

Dark purple powder. Yield 82%.

^{1}H NMR (300 MHz, Acetonitrile-d_3) δ 8.70 (s, 1H), 8.61 (d, *J* = 5.7 Hz, 1H), 8.33 (d, *J* = 8.2 Hz, 2H), 8.14 (d, *J* = 8.1 Hz, 1H), 8.04 (d, *J* = 8.1 Hz, 1H), 7.96 (d, *J* = 5.6 Hz, 1H), 7.88 – 7.78 (m, 3H), 7.76 – 7.68 (m, 3H), 7.66 (d, *J* = 5.3 Hz, 1H), 7.39 (t, *J* = 6.7 Hz, 1H), 7.30 (t, *J* = 6.7 Hz, 1H), 7.22 – 7.16 (m, 2H), 6.91 – 6.80 (m, 2H), 6.73 (d, *J* = 8.0 Hz, 2H), 6.52 (d, *J* = 7.1 Hz, 1H), 6.41 (d, *J* = 8.0 Hz, 2H), 2.12 (s, 3H).

^{13}C NMR (76 MHz, Acetonitrile-d3): 200.41, 174.77, 157.82, 157.03, 156.67, 154.60, 154.43, 152.31, 150.23, 149.08, 148.62, 148.44, 136.06, 135.78, 135.38, 135.05, 134.08, 133.79, 130.62, 128.91, 126.40, 126.17, 123.02, 122.70, 122.29, 121.47, 120.68, 117.36, 19.80.

CHN calc. for $C_{34}H_{28}N_5RuPF_6$: C: 54.26; H: 3.75; N: 9.30. Obs. C: 54.07; H: 3.70; N: 9.34.

Bis(2,2′-bipiridine)[N-((phenyl-κC^2)methyliden]-4-ethylaniline-κN]ruthenium(II) hexafluorophosphate (**3d**).

Dark purple powder. Yield 85%.

^{1}H NMR (300 MHz, Acetonitrile-d_3) δ 8.71 (s, 1H), 8.62 (d, *J* = 5.5 Hz, 1H), 8.33 (d, *J* = 8.3 Hz, 2H), 8.12 (d, *J* = 8.1 Hz, 1H), 8.02 – 7.95 (m, 2H), 7.89 – 7.78 (m, 3H), 7.76 – 7.63 (m, 4H), 7.39 (ddd, *J* = 7.3, 5.7, 1.4 Hz, 1H), 7.30 (ddd, *J* = 7.3, 5.7, 1.4 Hz, 1H), 7.19 (ddd, *J* = 7.5, 6.0, 1.1 Hz, 2H), 6.89 (td, *J* = 7.3, 1.5 Hz, 1H), 6.83 (td, *J* = 7.2, 1.7 Hz, 1H), 6.76 – 6.71 (m, 2H), 6.56 – 6.51 (m, 1H), 6.41 – 6.36 (m, 2H), 2.42 (q, *J* = 7.6 Hz, 2H), 1.05 (t, *J* = 7.6 Hz, 3H).

 doi:10.20944/preprints202512.0562.v1

^{13}C NMR (76 MHz, Acetonitrile-d_3): 200.43, 174.66, 157.85, 157.04, 156.66, 154.40, 152.33, 150.29, 149.07, 148.48, 142.53, 135.77, 135.33, 135.05, 134.04, 133.76, 130.61, 129.01, 127.76, 126.40, 126.15, 123.03, 122.63, 122.22, 121.52, 120.64, 117.35, 27.80, 15.28.

CHN calc. for $C_{35}H_{30}N_5RuPF_6$: C: 54.66; H: 3.94; N: 9.31. Obs. C: 54.87; H: 3.93; N :9.13.

Bis(2,2′-bipiridine)[N-((phenyl-κC²)methyliden]-4-(tert-butyl)aniline-κN]ruthenium(II) hexafluorophosphate (**3e**).

Dark purple powder. Yield 78%.

^{1}H NMR (300 MHz, Acetonitrile-d_3) δ 8.71 (s, 1H), 8.64 (d, *J* = 5.8 Hz, 1H), 8.34 (d, *J* = 8.1 Hz, 2H), 8.09 (d, *J* = 8.1 Hz, 1H), 7.98 (d, *J* = 5.7 Hz, 1H), 7.94 (d, *J* = 8.1 Hz, 1H), 7.89 – 7.77 (m, 4H), 7.73 (d, *J* = 7.3 Hz, 1H), 7.67 (t, *J* = 7.8 Hz, 1H), 7.62 (d, *J* = 5.3 Hz, 1H), 7.39 (t, *J* = 6.6 Hz, 1H), 7.30 (t, *J* = 6.6 Hz, 1H), 7.19 (q, *J* = 6.0 Hz, 2H), 6.92 – 6.81 (m, 4H), 6.55 (d, *J* = 7.2 Hz, 1H), 6.33 (d, *J* = 8.0 Hz, 2H), 1.15 (s, 9H).

^{13}C NMR (76 MHz, Acetonitrile-d_3): 205.61, 179.79, 163.22, 162.35, 161.97, 159.96, 159.68, 157.66, 155.67, 154.44, 154.39, 153.81, 153.10, 141.05, 140.62, 140.38, 139.31, 139.03, 135.87, 134.34, 131.42, 130.49, 128.36, 127.86, 127.48, 126.43, 125.94, 122.66, 39.21, 35.77.

CHN calc. for $C_{37}H_{34}N_5PF_6Ru$: C: 55.92; H: 3.84; N: 8.73. Obs. C: 55.90; H: 4.24; N :9.10.

Bis(2,2′-bipiridine)[N-((phenyl-κC²)methyliden]-4-methoxyaniline-κN]ruthenium(II) hexafluorophosphate (**3f**).

Dark purple powder. Yield 84%.

^{1}H NMR (300 MHz, Acetonitrile-d_3) δ 8.69 (s, 1H), 8.60 (d, *J* = 5.0 Hz, 1H), 8.33 (d, *J* = 8.2 Hz, 2H), 8.14 (d, *J* = 8.1 Hz, 1H), 8.05 (d, *J* = 8.2 Hz, 1H), 7.98 – 7.94 (m, 1H), 7.88 – 7.78 (m, 3H), 7.76 – 7.70 (m, 3H), 7.68 – 7.65 (m, 1H), 7.39 (ddd, *J* = 7.3, 5.7, 1.4 Hz, 1H), 7.30 (ddd, *J* = 7.4, 5.7, 1.4 Hz, 1H), 7.23 – 7.16 (m, 2H), 6.88 (td, *J* = 7.2, 1.5 Hz, 1H), 6.82 (td, *J* = 7.2, 1.7 Hz, 1H), 6.55 – 6.50 (m, 1H), 6.45 (s, 4H), 3.62 (s, 3H).

^{13}C NMR (151 MHz, Acetonitrile-d_3): 200.28, 174.42, 157.92, 157.83, 157.07, 156.71, 154.68, 154.42, 152.33, 150.31, 149.09, 148.46, 144.23, 135.82, 135.32, 135.04, 134.08, 133.78, 130.53, 128.94, 126.45, 126.19, 123.06, 122.71, 120.66, 117.37, 113.52, 55.12.

CHN calc. for $C_{34}H_{28}N_5ORuPF_6$: C: 53.13; H: 3.67; N: 9.11. Obs. C: 52.87; H: 3.76; N: 9.17.

Bis(2,2′-bipiridine)[N-((phenyl-κC²)methyliden]-4-ethoxycarbonylaniline-κN]ruthenium(II) hexafluorophosphate (**3g**).

Dark purple powder. Yield 75%.

^{1}H NMR (300 MHz, Acetonitrile-d_3) δ 8.78 (s, 1H), 8.60 (dd, *J* = 5.7, 0.7 Hz, 1H), 8.34 (dq, *J* = 8.2, 1.2 Hz, 2H), 8.14 (d, *J* = 8.0 Hz, 1H), 8.02 (d, *J* = 8.2 Hz, 1H), 7.97 – 7.94 (m, 1H), 7.90 – 7.78 (m, 4H), 7.73 – 7.65 (m, 3H), 7.57 – 7.52 (m, 2H), 7.40 (ddd, *J* = 7.3, 5.7, 1.4 Hz, 1H), 7.32 (ddd, *J* = 7.3, 5.7, 1.4 Hz, 1H), 7.24 – 7.17 (m, 2H), 6.91 (td, *J* = 7.3, 1.5 Hz, 1H), 6.86 (td, *J* = 7.3, 1.7 Hz, 1H), 6.63 – 6.56 (m, 3H), 4.25 (q, *J* = 7.1 Hz, 2H), 1.30 (t, *J* = 7.1 Hz, 3H).

^{13}C NMR (76 MHz, Acetonitrile-d_3): 201.83, 176.20, 165.42, 157.69, 157.00, 156.65, 154.68, 154.52, 152.36, 150.30, 149.12, 148.29, 135.94, 135.50, 135.29, 134.32, 134.01, 131.44, 129.69, 129.41, 128.07, 126.62, 126.25, 123.10, 122.82, 122.38, 122.02, 120.77, 117.35, 60.92, 13.54.

CHN calc. for $C_{36}H_{30}N_5O_2RuPF_6$*0.16$CHCl_3$: C: 52.13; H:3.88; N: 8.71. Obs. C: 52.40; H:3.84; N: 8.73.

Bis(2,2′-bipiridine)[N-((phenyl-κC²)methyliden]-4-nitroaniline-κN]ruthenium(II) hexafluorophosphate (**3h**).

Dark purple powder. Yield 79%.

^{1}H NMR (300 MHz, Acetonitrile-d_3) δ 8.85 – 8.78 (m, 1H), 8.60 – 8.53 (m, 1H), 8.38 – 8.31 (m, 2H), 8.15 – 8.09 (m, 1H), 8.04 – 7.98 (m, 1H), 7.93 (t, *J* = 5.6 Hz, 1H), 7.90 – 7.79 (m, 4H), 7.77 – 7.64 (m, 5H), 7.43 – 7.36 (m, 1H), 7.33 (t, *J* = 6.6 Hz, 1H), 7.27 – 7.17 (m, 2H), 6.96 – 6.83 (m, 2H), 6.72 – 6.64 (m, 2H), 6.63 – 6.57 (m, 1H).

^{13}C NMR (151 MHz, Acetonitrile-d_3): 202.80, 177.17, 157.64, 157.02, 156.67, 156.18, 154.60, 154.42, 152.42, 150.40, 149.12, 148.25, 145.46, 136.15, 135.60, 135.46, 134.51, 134.19, 131.98, 129.73, 126.87, 126.72, 126.50, 126.31, 124.05, 123.20, 123.16, 122.95, 122.60, 120.87, 117.35.

 doi:10.20944/preprints202512.0562.v1

CHN calc. for $C_{33}H_{25}N_6O_2PF_6Ru$*0.44$CHCl_3$*0.34$C_4H_{10}O$: C: 48.51; H: 3.38; N: 9.75. Obs. C: 48.51; H: 3.21; N :9.75.

Bis(2,2′-bipiridine)[N-((phenyl-κC^2)methyliden]-4-(trifluoromethyl)aniline-κN]ruthenium(II) hexafluorophosphate (**3i**).

Dark purple powder. Yield 82%.

^{1}H NMR (300 MHz, Acetonitrile-d_3) δ 8.78 (s, 1H), 8.59 (d, *J* = 5.7 Hz, 1H), 8.34 (d, *J* = 8.1 Hz, 2H), 8.13 (d, *J* = 8.1 Hz, 1H), 8.02 – 7.95 (m, 2H), 7.91 – 7.78 (m, 4H), 7.74 – 7.63 (m, 3H), 7.40 (t, *J* = 6.7 Hz, 1H), 7.33 (t, *J* = 6.7 Hz, 1H), 7.25 – 7.17 (m, 4H), 6.89 (q, *J* = 6.6 Hz, 2H), 6.64 (d, *J* = 8.0 Hz, 2H), 6.59 (d, *J* = 6.9 Hz, 1H).

^{13}C NMR (76 MHz, Acetonitrile-d_3): 201.70, 176.46, 157.69, 157.00, 156.63, 154.57, 152.34, 150.34, 149.16, 148.27, 135.92, 135.52, 135.34, 135.27, 134.34, 134.04, 131.46, 129.48, 126.64, 126.42, 126.24, 125.65, 123.11, 122.82, 122.53, 122.33, 120.80, 117.34.

CHN calc. for $C_{34}H_{25}N_5RuPF_9$*0.16CH_3CN: C: 50.47; H: 3.15; N: 8.85. Obs. C: 50.47; H: 3.15; N: 8.84.

Bis(2,2′-bipiridine)[N-((thiophene-2-yl-κC^2)methyliden]-4-fluoroaniline-κN]ruthenium(II) hexafluorophosphate (**3j**).

Dark purple powder. Yield 82%.

^{1}H NMR (300 MHz, Acetonitrile-d_3) δ 8.64 (s, 1H), 8.51 (d, *J* = 4.9 Hz, 1H), 8.32 (d, *J* = 8.1 Hz, 2H), 8.14 (d, *J* = 8.0 Hz, 1H), 8.07 (d, *J* = 8.2 Hz, 1H), 7.91 – 7.71 (m, 6H), 7.68 (d, *J* = 4.7 Hz, 1H), 7.61 (d, *J* = 4.7 Hz, 1H), 7.41 (ddd, 1H), 7.31 (ddd, 1H), 7.26 – 7.16 (m, 2H), 6.68 – 6.58 (m, 2H), 6.51 – 6.43 (m, 3H).

^{13}C NMR (76 MHz, Acetonitrile-d_3) δ 212.13, 166.43, 162.82, 159.60, 158.52, 158.39, 157.85, 155.74, 155.42, 153.95, 151.77, 150.03, 148.60, 148.56, 138.59, 136.93, 136.22, 135.82, 135.46, 135.18, 134.74, 127.58, 127.50, 127.31, 127.16, 124.61, 124.50, 124.03, 123.85, 123.69, 123.38, 116.06, 115.76.

CHN calc. for $C_{31}H_{23}F_7N_5OPRuS$: C: 48.82; H: 3.04; N: 9.18 Obs. C: 48.83; H: 3.04; N: 9.18.

Bis(2,2′-bipiridine)[N-((thiophene-2-yl-κC^2)methyliden]-4-methylaniline-κN]ruthenium(II) hexafluorophosphate (**3k**).

Dark purple powder. Yield 80%.

^{1}H NMR (300 MHz, Acetonitrile-d_3) δ 8.63 (s, 1H), 8.53 (d, *J* = 5.7 Hz, 1H), 8.31 (d, *J* = 8.1 Hz, 2H), 8.14 (d, *J* = 8.0 Hz, 1H), 8.06 (d, *J* = 8.1 Hz, 1H), 7.90 – 7.69 (m, 6H), 7.67 – 7.63 (m, 1H), 7.61 (d, *J* = 5.4 Hz, 1H), 7.44 – 7.36 (m, 1H), 7.33 – 7.26 (m, 1H), 7.19 (q, 2H), 6.71 (d, *J* = 8.1 Hz, 2H), 6.45 (d, *J* = 4.6 Hz, 1H), 6.39 (d, *J* = 8.3 Hz, 2H), 2.11 (s, 3H).

^{13}C NMR (76 MHz, Acetonitrile-d_3) δ 211.31, 165.81, 158.60, 158.40, 157.88, 155.77, 155.43, 153.94, 151.67, 149.99, 138.53, 136.81, 136.32, 136.08, 135.36, 135.33, 135.08, 134.70, 129.90, 127.44, 127.37, 127.28, 127.16, 123.99, 123.80, 123.65, 123.34, 122.66, 20.75.

CHN calc. for $C_{32}H_{26}F_6N_5PRuS$: C: 50.66; H: 3.45; N: 9.23 Obs. C: 50.48; H: 3.48; N: 9.20.

Bis(2,2′-bipiridine)[N-((thiophene-2-yl-κC^2)methyliden]-4-methoxyaniline-κN]ruthenium(II) hexafluorophosphate (**3l**).

Dark purple powder. Yield 77%.

^{1}H NMR (300 MHz, Acetonitrile-d_3) δ 8.61 (s, 1H), 8.53 (d, *J* = 4.9 Hz, 1H), 8.31 (d, *J* = 8.1 Hz, 2H), 8.14 (d, *J* = 8.1 Hz, 1H), 8.06 (d, *J* = 8.2 Hz, 1H), 7.90 – 7.70 (m, 6H), 7.64 (d, *J* = 4.6 Hz, 1H), 7.61 (d, *J* = 4.6 Hz, 1H), 7.40 (ddd, *J* = 7.3, 5.7, 1.4 Hz, 1H), 7.30 (ddd, *J* = 7.3, 5.7, 1.4 Hz, 1H), 7.25 – 7.15 (m, 2H), 6.45 (d, *J* = 4.6 Hz, 1H), 6.42 (br.s, 3H), 3.61 (s, 3H).

^{13}C NMR (76 MHz, Acetonitrile-d_3) δ 210.71, 165.46, 158.59, 158.44, 158.41, 157.88, 155.82, 155.39, 153.93, 151.72, 149.99, 145.56, 138.48, 136.82, 136.06, 135.32, 135.10, 135.04, 134.66, 127.45, 127.37, 127.27, 127.13, 123.99, 123.81, 123.61, 123.32, 114.48, 56.03, 15.64.

CHN calc. for $C_{32}H_{26}F_6N_5OPRuS$: C: 49.61; H: 3.38; N: 9.04 Obs. C: 49.60; H: 3.39; N: 9.08.

Bis(2,2′-bipiridine)[N-((thiophene-2-yl-κC^2)methyliden]-4-ethoxycarbonylaniline-κN]ruthenium(II) hexafluorophosphate (**3m**).

Dark purple powder. Yield 77%.

^{1}H NMR (300 MHz, Acetonitrile-d_3) δ 8.72 (s, 1H), 8.50 (d, *J* = 4.9 Hz, 1H), 8.33 (d, *J* = 8.4 Hz, 2H), 8.13 (d, *J* = 8.1 Hz, 1H), 8.05 (d, *J* = 8.2 Hz, 1H), 7.92 – 7.70 (m, 7H), 7.63 (d, *J* = 4.7 Hz, 1H), 7.55 – 7.49

 doi:10.20944/preprints202512.0562.v1

(m, 2H), 7.42 (ddd, *J* = 7.3, 5.7, 1.4 Hz, 1H), 7.32 (ddd, *J* = 7.3, 5.7, 1.4 Hz, 1H), 7.25 (ddd, *J* = 7.5, 5.4, 1.2 Hz, 1H), 7.19 (ddd, *J* = 7.3, 5.7, 1.4 Hz, 1H), 6.63 – 6.56 (m, 2H), 6.49 (d, *J* = 4.6 Hz, 1H), 4.24 (q, *J* = 7.1 Hz, 2H), 1.29 (t, *J* = 7.1 Hz, 3H).

^{13}C NMR (76 MHz, Acetonitrile-*d*$_3$) δ 166.89, 166.51, 158.46, 158.41, 157.89, 156.34, 155.61, 155.45, 154.08, 151.80, 150.05, 137.02, 136.80, 136.35, 135.63, 135.37, 134.88, 130.66, 128.29, 127.70, 127.53, 127.36, 127.25, 124.07, 123.90, 123.76, 123.46, 123.19, 61.80, 14.52.

CHN calc. for $C_{34}H_{28}F_6N_5O_2PRuS$: C: 50.00; H: 3.46; N: 8.57 Obs. C: 50.03; H: 3.48; N: 8.56.

Bis(2,2′-bipiridine)[N-((thiophene-2-yl-κC^2)methyliden]-4-nitroaniline-κN]ruthenium(II) hexafluorophosphate (**3n**).

Dark purple powder. Yield 65%.

^{1}H NMR (300 MHz, Acetonitrile-*d*$_3$) δ 8.78 (s, 1H), 8.48 (d, *J* = 5.6 Hz, 1H), 8.34 (d, *J* = 7.6 Hz, 2H), 8.12 (d, *J* = 8.0 Hz, 1H), 8.05 (d, *J* = 8.2 Hz, 1H), 7.95 – 7.71 (m, 9H), 7.64 (d, *J* = 5.3 Hz, 1H), 7.43 (t, *J* = 6.6 Hz, 1H), 7.35 – 7.26 (m, 2H), 7.20 (t, *J* = 6.7 Hz, 1H), 6.68 (d, *J* = 9.0 Hz, 2H), 6.52 (d, *J* = 4.7 Hz, 1H).

^{13}C NMR (76 MHz, Acetonitrile-*d*$_3$) δ 217.12, 167.65, 158.41, 158.36, 158.11, 157.88, 155.48, 155.42, 154.14, 151.90, 149.98, 145.73, 139.52, 137.86, 137.24, 136.52, 135.82, 135.56, 135.02, 127.96, 127.64, 127.43, 127.30, 125.02, 124.13, 124.00, 123.95, 123.86, 123.67.

CHN calc. for $C_{31}H_{23}F_6N_6O_2PRuS$: C: 47.15; H: 2.94; N: 10.64 Obs. C: 46.99; H: 2.96; N: 10.61.

Bis(2,2′-bipiridine)[N-((thiophene-2-yl-κC^2)methyliden]-4-(trifluoromethyl)aniline-κN]ruthenium(II) hexafluorophosphate (**3o**).

Dark purple powder. Yield 96%.

^{1}H NMR (300 MHz, Acetonitrile-*d*$_3$) δ 8.73 (s, 1H), 8.51 (d, *J* = 4.9 Hz, 1H), 8.33 (d, *J* = 7.2 Hz, 2H), 8.13 (d, *J* = 8.1 Hz, 1H), 8.04 (d, *J* = 8.2 Hz, 1H), 7.93 – 7.70 (m, 7H), 7.62 (d, *J* = 4.8 Hz, 1H), 7.42 (ddd, *J* = 7.4, 5.7, 1.4 Hz, 1H), 7.32 (ddd, *J* = 7.3, 5.7, 1.4 Hz, 1H), 7.27 – 7.17 (m, 4H), 6.63 (d, *J* = 8.0 Hz, 2H), 6.51 (d, *J* = 4.7 Hz, 1H).

^{13}C NMR (76 MHz, Acetonitrile-*d*$_3$) δ 214.53, 167.20, 158.45, 158.41, 157.87, 155.63, 155.49, 155.38, 154.06, 151.82, 150.06, 139.05, 137.01, 136.87, 136.40, 135.65, 135.38, 134.87, 127.73, 127.59, 127.37, 127.23, 126.64, 126.59, 126.54, 126.48, 124.09, 123.92, 123.76, 123.71, 123.41.

CHN calc. for $C_{32}H_{23}F_9N_5PRuS$: C: 47.30; H: 2.85; N: 8.62 Obs. C: 47.28; H: 2.79; N: 8.63.

4. Conclusions

Two bisheteroleptic ruthenium(II) compounds containing different types of the simplest cyclometallated imines of 2-thiophenecarboxaldehyde and benzaldehyde were synthesized and characterized by NMR, MS, elemental analysis and UV-vis spectroscopy and cyclic voltammetry. The structure of 22 complexes described was proved by means of single crystal X-ray data. Cytotoxic activity was measured on two cancer and one non-cancerous cell line, and the proportion of cell death was measured using the MTT assay. The cytotoxicity of all ruthenium complexes is significantly higher than that of cisplatin, but they have less selectivity.

Supplementary Materials: The following supporting information can be downloaded at: Preprints.org, Experimental details: pp. S2-S4; NMR spectra: pp. S5-S34; Crystallography: pp S35-S52; Stability in PBS: pp S53-S54.

Author Contributions: Conceptualization Vasil'ev A.A., Medved'ko A.V.; investigation, Vasil'ev A.A., Troshin A.I., Shangin P.G., Voroshilkina K.M., Shutkov I.A., Medved'ko A.V.; writing—original draft preparation, Vasil'ev A.A., Troshin A.I.; writing—Nazarov A.A., Medved'ko A.V.; funding acquisition, Medved'ko A.V. All authors have read and agreed to the published version of the manuscript.

Funding: This research was funded by Russian Science Foundation, grant number 24-23-00066

Institutional Review Board Statement: Not applicable.

Data Availability Statement: Data is contained within the article or supplementary material.

 doi:10.20944/preprints202512.0562.v1

Acknowledgments: Crystal structure determination was performed in the Department of Structural Studies of Zelinsky Institute of Organic Chemistry, Moscow. The authors acknowledge support from the M.V. Lomonosov Moscow State University Program of Development («Feyond-A400» microplate reader (Allsheng, China)) and automated pipetting system «EzMate» (Blue-Ray Biotech , Taiwan).

Conflicts of Interest: The authors declare no conflicts of interest

References

1. Oun, R.; Moussa, Y.E.; Wheate, N.J. The Side Effects of Platinum-Based Chemotherapy Drugs: A Review for Chemists. *Dalt. Trans.* **2018**, *47*, 6645–6653, doi:10.1039/C8DT00838H.
2. Barabas, K.; Milner, R.; Lurie, D.; Adin, C. Cisplatin: A Review of Toxicities and Therapeutic Applications. *Vet. Comp. Oncol.* **2008**, *6*, 1–18, doi:10.1111/j.1476-5829.2007.00142.x.
3. Deo, K.; Pages, B.; Ang, D.; Gordon, C.; Aldrich-Wright, J. Transition Metal Intercalators as Anticancer Agents—Recent Advances. *Int. J. Mol. Sci.* **2016**, *17*, 1818, doi:10.3390/ijms17111818.
4. Adhikari, S.; Nath, P.; Das, A.; Datta, A.; Baildya, N.; Duttaroy, A.K.; Pathak, S. A Review on Metal Complexes and Its Anti-Cancer Activities: Recent Updates from in Vivo Studies. *Biomed. Pharmacother.* **2024**, *171*, 116211, doi:10.1016/j.biopha.2024.116211.
5. Alessio, E.; Messori, L. NAMI-A and KP1019/1339, Two Iconic Ruthenium Anticancer Drug Candidates Face-to-Face: A Case Story in Medicinal Inorganic Chemistry. *Molecules* **2019**, *24*, 1995, doi:10.3390/molecules24101995.
6. Weiss, A.; Berndsen, R.H.; Dubois, M.; Müller, C.; Schibli, R.; Griffioen, A.W.; Dyson, P.J.; Nowak-Sliwinska, P. In Vivo Anti-Tumor Activity of the Organometallic Ruthenium(Ii)-Arene Complex [Ru(η 6 - p -Cymene)Cl 2 (Pta)] (RAPTA-C) in Human Ovarian and Colorectal Carcinomas. *Chem. Sci.* **2014**, *5*, 4742–4748, doi:10.1039/C4SC01255K.
7. McKenzie, L.K.; Bryant, H.E.; Weinstein, J.A. Transition Metal Complexes as Photosensitisers in One- and Two-Photon Photodynamic Therapy. *Coord. Chem. Rev.* **2019**, *379*, 2–29, doi:10.1016/j.ccr.2018.03.020.
8. Shi, G.; Monro, S.; Hennigar, R.; Colpitts, J.; Fong, J.; Kasimova, K.; Yin, H.; DeCoste, R.; Spencer, C.; Chamberlain, L.; et al. Ru(II) Dyads Derived from α-Oligothiophenes: A New Class of Potent and Versatile Photosensitizers for PDT. *Coord. Chem. Rev.* **2015**, *282–283*, 127–138, doi:10.1016/j.ccr.2014.04.012.
9. Green, M.A.; Emery, K.; Hishikawa, Y.; Warta, W.; Dunlop, E.D. Solar Cell Efficiency Tables (Version 46). *Prog. Photovoltaics Res. Appl.* **2015**, *23*, 805–812, doi:10.1002/pip.2637.
10. Chang, X.; Chuan, L.W.; Yongxin, L.; Pullarkat, S.A. One-Pot β-Alkylation of Secondary Alcohols with Primary Alcohols Catalyzed by Ruthenacycles. *Tetrahedron Lett.* **2012**, *53*, 1450–1455, doi:10.1016/j.tetlet.2012.01.025.
11. Findlay, M.T.; Domingo-Legarda, P.; McArthur, G.; Yen, A.; Larrosa, I. Catalysis with Cycloruthenated Complexes. *Chem. Sci.* **2022**, *13*, 3335–3362, doi:10.1039/d1sc06355c.
12. Lin, K.; Zhao, Z.Z.; Bo, H. Ben; Hao, X.J.; Wang, J.Q. Applications of Ruthenium Complex in Tumor Diagnosis and Therapy. *Front. Pharmacol.* **2018**, *9*, 1–10, doi:10.3389/fphar.2018.01323.
13. Parveen, S. Recent Advances in Anticancer Ruthenium Schiff Base Complexes. *Appl. Organomet. Chem.* **2020**, *34*, 1–23, doi:10.1002/aoc.5687.
14. Gaiddon, C.; Pfeffer, M. The Fate of Cycloruthenated Compounds: From C–H Activation to Innovative Anticancer Therapy. *Eur. J. Inorg. Chem.* **2017**, *2017*, 1639–1654, doi:10.1002/ejic.201601216.
15. Li, J.; Zeng, L.; Wang, Z.; Chen, H.; Fang, S.; Wang, J.; Cai, C.Y.; Xing, E.; Liao, X.; Li, Z.W.; et al. Cycloruthenated Self-Assembly with Metabolic Inhibition to Efficiently Overcome Multidrug Resistance in Cancers. *Adv. Mater.* **2022**, *34*, doi:10.1002/adma.202100245.
16. Sui, L.Z.; Yang, W.W.; Yao, C.J.; Xie, H.Y.; Zhong, Y.W. Charge Delocalization of 1,4-Benzenedicyclometalated Ruthenium: A Comparison between Tris-Bidentate and Bis-Tridentate Complexes. *Inorg. Chem.* **2012**, *51*, 1590–1598, doi:10.1021/ic202295b.
17. Cuesta, L.; Maluenda, I.; Soler, T.; Navarro, R.; Urriolabeitia, E.P. Novel Thiophene-Based Cycloruthenated Compounds: Synthesis, Characterization, and Reactivity. *Inorg. Chem.* **2011**, *50*, 37–45, doi:10.1021/ic101946n.

 doi:10.20944/preprints202512.0562.v1

18. Gaiddon, C.; Jeannequin, P.; Bischoff, P.; Pfeffer, M.; Sirlin, C.; Loeffler, J.P. Ruthenium (II)-Derived Organometallic Compounds Induce Cytostatic and Cytotoxic Effects on Mammalian Cancer Cell Lines through P53-Dependent and P53-Independent Mechanisms. *J. Pharmacol. Exp. Ther.* **2005**, *315*, 1403–1411, doi:10.1124/jpet.105.089342.
19. Matsui, T.; Sugiyama, H.; Nakai, M.; Nakabayashi, Y. DNA Interaction and Cytotoxicity of Cyclometalated Ruthenium(II) Complexes as Potential Anticancer Drugs. *Chem. Pharm. Bull. (Tokyo).* **2016**, *64*, 282–286, doi:10.1248/cpb.c15-00903.
20. Peña, B.; David, A.; Pavani, C.; Baptista, M.S.; Pellois, J.P.; Turro, C.; Dunbar, K.R. Cytotoxicity Studies of Cyclometallated Ruthenium(II) Compounds: New Applications for Ruthenium Dyes. *Organometallics* **2014**, *33*, 1100–1103, doi:10.1021/om500001h.
21. Riegel, G.; Orvain, C.; Recberlik, S.; Spaety, M.-E.; Poschet, G.; Venkatasamy, A.; Yamamoto, M.; Nomura, S.; Tsukamoto, T.; Masson, M.; et al. The Unfolded Protein Response-Glutathione Metabolism Axis: A Novel Target of a Cycloruthenated Complexes Bypassing Tumor Resistance Mechanisms. *Cancer Lett.* **2024**, *585*, 216671, doi:10.1016/j.canlet.2024.216671.
22. Medved'ko, A.V.; Ivanov, V.K.; Kiskin, M.A.; Sadovnikov, A.A.; Apostolova, E.S.; Grinberg, V.A.; Emets, V.V.; Chizhov, A.O.; Nikitin, O.M.; Magdesieva, T.V.; et al. The Design and Synthesis of Thiophene-Based Ruthenium(II) Complexes as Promising Sensitizers for Dye-Sensitized Solar Cells. *Dye. Pigment.* **2017**, *140*, 169–178, doi:10.1016/j.dyepig.2017.01.030.
23. Medved'ko, A. V.; Vasil'ev, A.A.; Kiskin, M.A.; Syroeshkin, M.A.; Balycheva, V.A.; Melnichuk, N.A.; Nazarov, A.A.; Vatsadze, S.Z. Cycloruthenated Thiophene-Imines: Novel Anticancer Agents. *J. Organomet. Chem.* **2025**, *1038*, 123726, doi:10.1016/j.jorganchem.2025.123726.
24. Su, X.; Zeng, R.; Li, X.; Dang, W.; Yao, K.; Tang, D. Cycloruthenated Complexes: PH-Dependent Reversible Cyclometallation and Reactions with Nitrite at Octahedral Ruthenium Centers. *Dalt. Trans.* **2016**, *45*, 7450–7459, doi:10.1039/C6DT00576D.